



## Research papers

## Near-inertial motions in the Brazil Current at 24°S–36°S: Observations by satellite tracked drifters

Arcilan T. Assireu<sup>a,\*</sup>, Thibaut Dauhut<sup>b</sup>, Francisco A. dos Santos<sup>c</sup>, João A. Lorenzzetti<sup>d</sup><sup>a</sup> Natural Resources Institute, Federal University of Itajubá, Itajubá, 37500-903 Minas Gerais, Brazil<sup>b</sup> Laboratoire d'Aérodynamique, Université de Toulouse, CNRS, UPS, France<sup>c</sup> PROCCEANO Serviço Oceanográfico, 20030-003 Rio de Janeiro, Brazil<sup>d</sup> Remote Sense Division, National Institute for Space Research, São José dos Campos, 12227-010 São Paulo, Brazil

## ARTICLE INFO

## Keywords:

Near-inertial currents  
Brazil Current  
Drifters  
Submesoscale flow

## ABSTRACT

Increased spatial and temporal resolution of recent observations and modeling have pointed out the importance of small scale structures (in the range of 1–50 km) for the mixing processes in the ocean. Based on high-frequency drifter measurements, we show here that the near-inertial currents (NICs) can contribute significantly to the surface kinetic energy in the Brazil Current (BC) region and, therefore, should be properly taken into account in the studies of transport and mixing processes. To characterize these submesoscale features, we examine the current response to the wind forcing in the Brazilian ocean margin between 24°S and 36°S using 3-hourly sampled trajectories of satellite-tracked drifters. Our results indicate a preference for anti-cyclonic circular motions, with a rotating period close to the local inertial period, consistent with near-inertial motions in the Southern Hemisphere (SH). Wind stress time series, from three months of wind measurements, along with synoptic weather charts, are used to relate the observed NICs to the atmospheric forcing. During SH spring, NICs occur in 4.7–15 day bursts and account for 15–45% of the total surface current variance. This intermittency is related to atmospheric cold frontal passages, low pressure systems, and sea breeze/land breeze circulations. The predominance of NICs south of 28°S appears to be related to the increased Effective Inertial Frequency (EIF), which is the inertial frequency changed by the sub-inertial background flow.

## 1. Introduction

Near-inertial currents (NICs) are oscillating motions of water masses with a frequency close to the inertial frequency  $f$ . The inertial frequency depends on the latitude  $\varphi$ :  $f = 2 \Omega \sin \varphi$ , where  $\Omega = 7.3 \cdot 10^{-5} \text{ rad s}^{-1}$  is the Earth rotation rate. About half of the kinetic energy in the global ocean is associated with near-inertial currents, that generate energy fluxes comparable to the internal tides (Munk and Wunsch, 1998; Watanabe and Hibiya, 2002; Alford, 2003a, 2003b; Park et al., 2005; Alford et al., 2012). However, in the region of the Brazilian southeast and south continental shelf break, the NICs have periods of approximately one day, and they may be easily mistaken for currents generated by the dominant tidal constituents ( $O_1$  and  $K_1$ ). We use here the anticyclonic rotational signature of the NICs to distinguish them from tidal currents.

Many observational (D'Asaro, 1985; Hyder et al., 2007, 2011; Sobarzo et al., 2007), theoretical (Pollard, 1970, 1980; Kroll, 1975; Gill, 1984) and numerical studies (Munk and Wunsch, 1998; Zhang et al., 2010) have suggested that the wind is one of the primary energy

sources for the near-inertial currents in the ocean. Near-inertial motions can be driven by wind injections of momentum (Price, 1981; D'Asaro, 1985; Xing et al., 2004) or by periodic sea breeze in the regions where the diurnal forcing period and the NICs period are similar (Hyder et al., 2007, 2011; Zhang et al., 2010). Similar frequencies in the wind forcing and in the current response further leads to a resonance phenomenon: The closer the frequency of the forcing is to the inertial frequency, the more intense the NICs are. Considering the forcing by the sea breeze, Simpson et al. (2002), Hyder et al. (2007) and Hyder et al. (2011), among others, showed that such an inertial resonance can occur at 30°N/S, generating NICs characterized by anti-cyclonic circular motions. In a recent numerical modeling study, Zhang et al. (2010) pointed out the importance of the background water column vorticity in shifting to the north or to the south the resonant latitude with the sea-breeze forcing. The modification of the near-surface near-inertial currents by the background vorticity was also investigated by Elipot et al. (2010) indicating that resonant latitudes may not be limited to near 30° latitude.

The sea breeze can be strong in many regions close to 30°N/S and

\* Corresponding author.

E-mail address: [arcilan@unifei.edu.br](mailto:arcilan@unifei.edu.br) (A.T. Assireu).

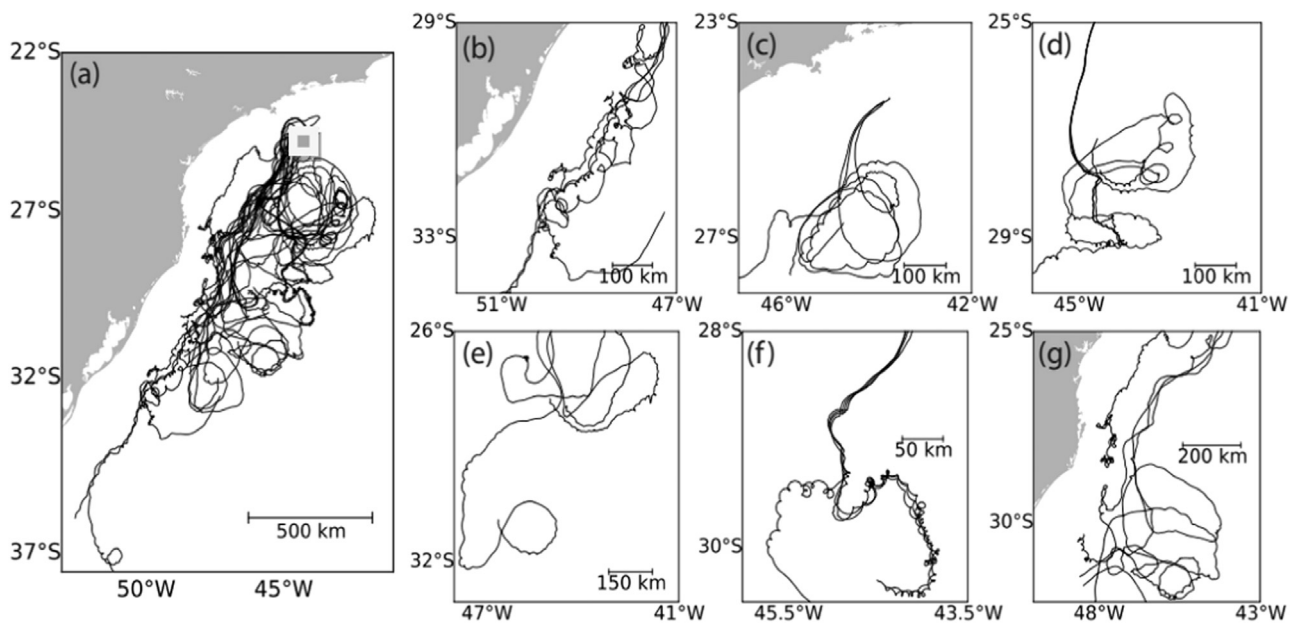


**Fig. 1.** Trajectories by satellite-tracked drifters launched in the SE/S Brazilian coast between September and November 2007 showing (a) segments for times of continuous tracking of the 39 drifters, and (b) detailed view of the drifter trajectories for time periods presenting near-inertial currents between September 15 and 25; (c) October 3 and 11; (d) October 16 and 22; (e) October 31 to November 10; (f) November 8 and 13 and (g) November 15 and 19. The gray box indicates the launching position of the drifters and the wind observational station.

may extend over the ocean quite far from the coast: it can be detected up to 300 km offshore at those latitudes (Gille et al., 2003, 2005). Sea breeze, with different magnitudes, is detectable over most Brazilian coastal regions. Particularly near 23°S, the seasonal coastal upwelling can strengthen the sea breeze signal, with day-night amplitude up to  $15 \text{ m s}^{-1}$  (Franchito et al., 1998). Much effort has been directed to study dynamical processes in the world's ocean associated with sea-breezes (e.g., Craig, 1989; Pattiaratchi et al., 1997; Chan and Xie, 1997; Hyder et al., 2007, 2011). There is however a near absence of observational studies for the Brazilian coastal waters. Franchito et al. (1998) suggested that there is a positive feedback between the sea-breeze and the coastal upwelling in the region of Cabo Frio (23°S, 42°W), but they did not discuss the dynamical link between the sea breeze and the diurnal currents. Stech and Lorenzetti (1992) used a barotropic model to study the response of the currents in the South Brazil Bight to the passage of cold fronts. These authors pointed out the inertial currents and their resonance with the diurnal winds.

The mixed layer inertial currents generated by wind propagate downward and promote vertical mixing through shear instability (Simpson et al., 2002; Rippeth et al., 2002). When the sea breeze is resonant with the inertial period of the ocean, the wind driving has an in-phase relationship with inertial current and continuously transfers energy into the ocean (Gill, 1984). This process is important to ocean vertical mixing. As an example, Zhang et al. (2010) showed that a  $4 \text{ m s}^{-1}$  sea breeze wind at 30°N deepens the 15 °C isotherm from 15 m to 25 m. Results from a numerical study by Furuichi et al. (2008) indicated that 85% of the near-inertial energy deposited into the mixed layer by the wind is dissipated in the upper 150 m. However, Alford et al. (2012) found that a substantial fraction of the energy input into the mixed layer reached 800 m. The work done by the wind on the mixed layer is computed as the dot product of the wind stress (from measured wind) and the mixed layer currents (Alford et al., 2012). The wind can thus both accelerate and decelerate the inertial currents (Pollard, 1980; D'Asaro, 1985).

Satellite-tracked drifters have been used to study the low-frequency basin-scale ocean circulation along the Brazilian coast. Some drifters deployed in the southwestern Atlantic (Assireu et al., 2003) revealed relevant seasonal differences in the mean conditions of the surface currents that are related to meteorological anomalies. Berti et al.

(2011) analyzed measurements from drifters deployed in this region. They found that the advection is modulated by the response of the currents to a wind forcing with a period about 6.5 days. Binning 13 years of surface drifter data onto a  $0.5^\circ \times 0.5^\circ$  grid, Oliveira et al. (2009) studied the mean surface circulation in the southwestern Atlantic. Their analysis of the kinetic energy conversion term suggested the presence of barotropic instabilities along the Brazil Current (BC). Using surface drifter data, Stevenson et al. (1998) and Souza and Robinson (2004) studied the intrusion of cold waters on the SE Brazilian inner shelf and concluded that local winds, blowing from the south, can contribute to the north-easterly flowing Brazilian Coastal Current. Despite the above results, which are focused on low-frequency processes, drifter measurements studies of the high-frequency variability, such as the near-inertial motions, are absent for the BC region.

In this paper, we use the trajectories of satellite-tracked surface drifters to examine the motions in the inertial frequency band. Three months of wind amplitude and direction measured at 10-m height in the drifters deployment region allow us to investigate the relationships between the local wind and the motions in the upper ocean. The relationship of the inertial events to the atmospheric conditions is investigated by examining synoptic weather charts. Together, the high-frequency drifter measurements (every 3 h), the offshore wind measurements (with a temporal interval of 10 min) and the daily synoptic weather charts enable us to describe, for the first time in the southwestern Atlantic, the geographical distribution of the near-inertial currents (NICs), their interaction with the sea-breeze and their modulation by the background vorticity of the Brazil Current.

The organization of the paper is as follows: Section 2 describes the dataset, Section 3 presents the results of the analysis, Section 4 discusses the spatial variability and intermittency of the NICs in terms of wind, resonant forcing and background flow vorticity, and Section 5 contains the main conclusions of the study.

## 2. Data set and methods

### 2.1. Study area and drifter data

An observational study based on surface currents measured by drifters, wind and synoptic meteorological conditions is designed in

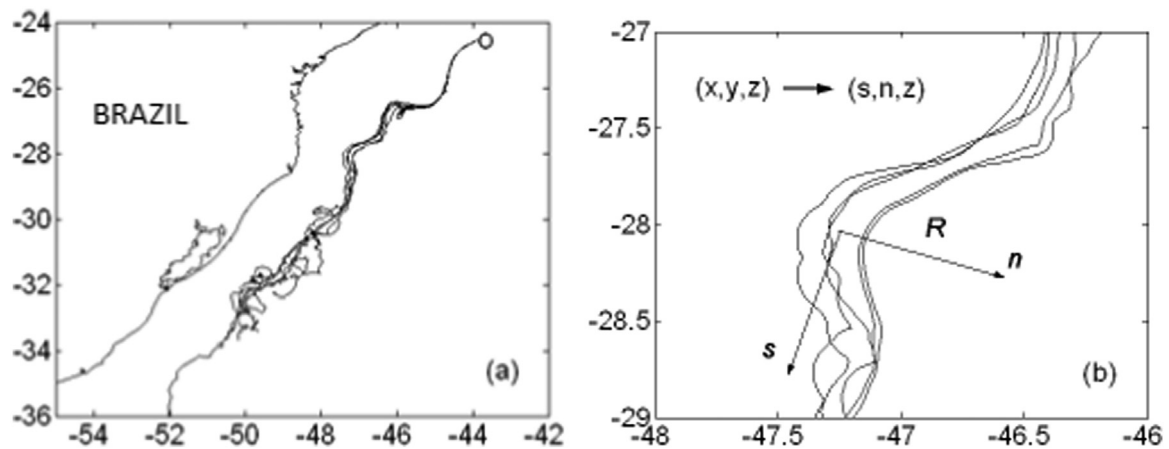


Fig. 2. (a) Some drifter trajectories along the coast and deployment position (empty dot); (b) Natural coordinate systems applied on drifter trajectories.

order to analyze the intermittency of the near-inertial currents along the Brazilian SE/S continental shelf. Our findings are based on 39 trajectories of surface drifters (drogued at 15 m) launched in the proximity to the Brazilian coast, around (24°S, 44°E) between September 2007 and November 2007 (Fig. 1a). Within the 39 drifters, 14 were deployed individually with a 3-day frequency and 25 were deployed in clusters of 5, every 12 days. A frequency of deployment of 3 days was set in order to perform at least 2 launches within the 6.5-day energy peak of the wind variability in the region (Stech and Lorenzetti, 1992). Each Lagrangian drifter used in this study had a drogue on/drogue off sensor used to determine if the drifter has lost its drogue. Out of 39 drifters two lost their drogues, so the set of useful drifters was reduced to 37 units. The observed southwestward surface drift (Fig. 1a) is consistent with the mean circulation pattern of the BC, with the hydrographic and numerical studies in the region (e.g., Silveira et al., 2000), as well as with the previous satellite-tracked drifter studies in the region (Assireu et al., 2003; Souza et al., 2004; Oliveira et al., 2009). The poleward BC is a relatively warm and saline western boundary current, with its core observed most of the time meandering over the 200-m isobaths (Peterson and Strama, 1991; Lima et al., 1996). The surface velocity inside the BC has values between 25 and 80  $\text{cm s}^{-1}$  (Castro Filho et al., 2006) and its volume flux increases with latitude (Müller et al., 1998; Gordon and Greengrove, 1986). Along their general southward displacements, and during some specific periods, some drifter trajectories showed characteristics of near-inertial currents (Fig. 1b-g).

The drifters used (MetOcean Instruments) have a drag area ratio (~45:1), following the design proposed by Sybrandt and Niiler (1991), which minimizes errors arising from slippage between water and drogue and from wind drag on the surface element of the drifter. Considering that the expected drifter position accuracy from the GPS system used by IRIDIUM tracking is  $\Delta x \sim 20$  m and 3-hourly sampling rate ( $\Delta t = 3$  h), the velocity errors  $v_e \sim \Delta x/\Delta t$  for the instantaneous velocity has a magnitude of less than  $0.5 \text{ cm s}^{-1}$ . The time between successive positions is short enough so that the Nyquist period (6 h) does not filter out the inertial motions in the studied region (periods between 20.9 and 29.5 h). Data used in this study have passed the quality control proposed by Hansen and Poulain (1996) in the Global Drifter Program (GPD) database.

## 2.2. Spectral analysis

The southward displacement of the drifters, related to the meridional excursion of the surface layer of BC, is expected to shift or to broaden the inertial peak. In order to minimize this effect, the spectral analysis is carried out on a composite of drifters dataset for each  $1^\circ$  latitude bandwidth. The data are transformed to a regular Cartesian

coordinate system centered on the mean latitude for each segment.

The relative importance of a rotary velocity field with respect to the other motions like the turbulent eddies can be examined by performing rotary spectral analyses. Although not initially designed for nonstationary processes and spatially heterogeneous flow, this method has been extensively applied to both current meter records and Lagrangian measurements (Gonella, 1972). The drifter's velocity records are Fourier transformed into a counterclockwise  $S^+(\omega)$  and a clockwise  $S^-(\omega)$  circular spectral components as detailed in Crawford et al. (1997). The rotary coefficient  $r$  ( $-1 \leq r \leq 1$ ), which indicates the strength and the sense of the rotary motions, is given in terms of the rotary spectra by  $r = (S^+ - S^-) / (S^+ + S^-)$ . It is positive (negative) for counterclockwise (clockwise) motions and equal to zero (unity) for rectilinear (circularly polarized) motions. We remark that the definition above differs in sign from that of Crawford et al. (1997) who used  $S^- - S^+$  rather than  $S^+ - S^-$  in the numerator. A linear trend is removed from each drifter velocity segment by fitting a straight line to each diurnal time window. In order to reduce the influence of sharp transitions in signal level between the ends of the records and to reduce the sidelobes, it is common to use tapered windows, as Kaiser-Bessel, Hanning, Bartlett, among others, prior to the Fourier transform. Such techniques applied to short-duration signals (in our case, mean duration of 10 days, 8 drifter position per day) broadens the peaks and thus reduces spectral resolution. A reasonable alternative to this is to select segments whose durations are integral multiples of periods of diurnal variability, as suggested by Crawford et al. (1997).

## 2.3. Relative vorticity

The upper-layer streamlines of BC along the SE/S Brazil coast have a strong curvature (Fig. 2a,b). In order to estimate the relative vorticity from drifter data, we used the five trajectories showed in Fig. 2a. The relative vorticity  $\zeta$  is conveniently determined from the expression in natural coordinates (Arthur, 1965):

$$\zeta = \frac{V}{R} - \frac{\partial V}{\partial n} \quad (1)$$

where  $V$  is the speed,  $R$  is the radius of curvature of the streamline, and  $\partial V/\partial n$  is the velocity gradient normal to the streamline (Fig. 2b). A tendency for counterclockwise rotation is positive by the convention of signs.

## 3. Results

### 3.1. Observations

As indicated in Fig. 3a, the 3-hourly sampling rate is sufficient to

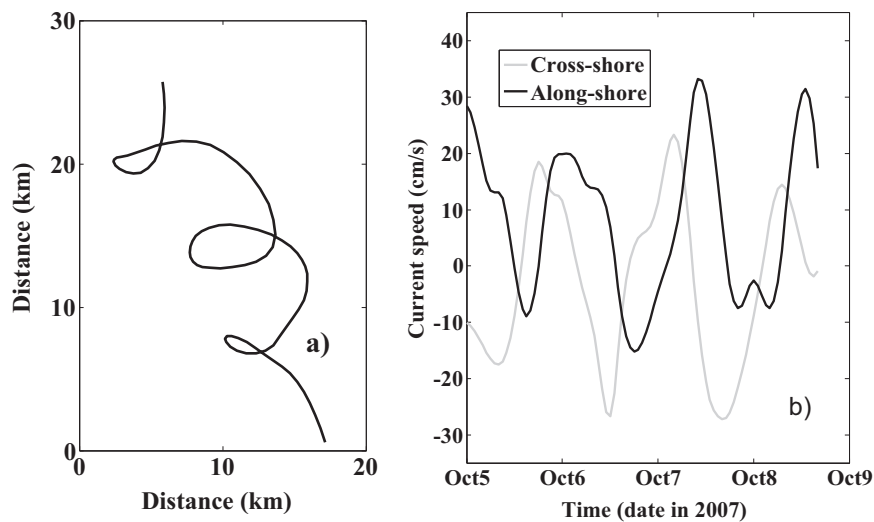


Fig. 3. (a) Detailed view of typical near inertial motions showed by the drifter trajectories; (b) Along-shore (black) and cross-shore (gray) current.

delineate the small-scale displacement due to the near-inertial motions. Based on the observed values of diameters ( $d \sim 1\text{--}5$  km), the velocity of the circularly polarized inertial currents can be estimated with  $\pi d/T_i \sim 3\text{--}20$  cm  $s^{-1}$ , in accordance with the values in Fig. 3b. Thomas et al. (2008) defined submesoscale flows, based on dynamics, as the flows where the Rossby number, defined by  $R_o = \zeta/f$ , is  $O(1)$ . Since  $\zeta \sim U/L$  and  $R_o = U/fL$ , applying the mean values observed ( $L \sim 3$  km,  $U \sim 10$  cm  $s^{-1}$  and  $f \sim 10^{-5}$   $s^{-1}$  in the studied region) gives  $R_o = O(1)$ . In terms of spatial scales, the length scale varies from 1 km to 42 km. These values are equivalent to the first internal Rossby radius of deformation in the region (Houry et al., 1987). In most cases, the near-inertial cross-shore  $u$  and along-shore  $v$  components have similar magnitudes and  $u$  leads  $v$  by a phase of approximately  $90^\circ$  (Fig. 3b), as expected for anticyclonic circular near-inertial currents.

The estimated mean amplitudes of the diurnal tidal currents in the upper (5–20 m) part of the water column are usually lower than 8 cm  $s^{-1}$  in our study area (Mesquita and Harari, 2003). The near-inertial currents excited by the winds can reach amplitudes as large as 30 cm  $s^{-1}$  (Fig. 3b). This implies that in the studied region, there is considerably less energy in the tidal band than in the near-inertial band in the upper ocean layer. Thus, the presence of near-inertial motions could be one of the most important factors in mixing across the pycnocline in our study area. This conclusion is identical to that presented by Jarosz et al. (2007) for the DeSoto Canyon region.

During the spring season, the winds in the SE Brazil Coast area are predominantly northeasterlies (Fig. 4a) as part of the western edge of the South Atlantic high pressure center. The alongshore orientation occurs about 75% of the time (cf. sum of NE and SW wind occurrences in Fig. 4a). The wind rotary spectrum is anti-cyclonically polarized with a pronounced near-inertial peak (Fig. 4b). As anticipated by some authors (e.g. Crawford and Large, 1996; Hyder et al., 2002; Hyder et al., 2011) a resonant response of the ocean to the wind forcing can occur when the wind stress presents a significant anticyclonic rotary spectral component at the inertial frequency.

For the energy analysis, the along-shore and cross-shore current components are detided and filtered (keeping harmonics with periods shorter than 40 h, i.e., frequencies larger than 0.6 cpd) in order to isolate the near-inertial variability. The counterclockwise component of the rotary spectra, related to the near-inertial peaks for all currents measured by drifters, shows values much larger than the clockwise component (e.g., Fig. 5b). This is consistent with inertial motions in the southern hemisphere. The current variability measured by the drifters is divided into three frequency bands (Fig. 5a): The low-frequency (LF) band (sub-inertial), with frequencies less than 0.8 cpd ( $T > 30$  h); the

inertial ( $f$ ) band, with frequencies between 0.8 and 1.1 cpd ( $21.8 \text{ h} < T < 30 \text{ h}$ ); and the high-frequency (HF) band, with frequencies greater than 1.1 cpd ( $T < 21.8 \text{ h}$ ). With the exception of the  $f$  band, the variance explained by the LF and HF are similar for data bins south of and north of  $28^\circ\text{S}$ . The sub-inertial winds (LF) are much less effective at generating near-inertial motions in the ocean (Xing et al., 2004). The motions in the  $f$  band account for 18% of the variance north of  $28^\circ\text{S}$  and for 45% of the variance south of  $28^\circ\text{S}$ . Considering the whole drifter trajectories, more than a quarter of the current variance is explained by the variability in the inertial  $f$  band.

### 3.2. The background vorticity

Fig. 6a displays a typical drifter trajectory, passing along the SE/S Brazilian coast. Most of the drifter tracks normally lies more than 100 km off the shore, over waters deeper than 500 m, which coincides with the space variability of the surface BC inshore front indicated by Lorenzetti et al. (2009).

The average relative vorticity ( $\zeta$ ), estimated from the low-passed currents, using Eq. (1) (Fig. 6b), ranges from  $-0.3f$  to  $0.4f$ . Using time series from ten moorings equipped with current-meters, Silveira et al. (2000) revealed that BC mean flow essentially follows the local 1000-m isobath. The amplitude of the meanders decays sharply with depth. As the drifters have a holey-sock drogue centered at 15 m depth, they were likely embedded in the most vigorous meanders of the surface layer. As a comparison, Nakamura and Kagimoto (2006) showed that the magnitude of  $\zeta$  ranges from 10% to 50% of  $f$  magnitude in the core of the Florida Current. The spectral analysis of the trajectories south of  $27.5^\circ\text{S}$  (Fig. 7) indicates that the near-inertial frequency is about 10% higher than the local inertial frequency, a blue frequency shift. In the northern portion (north of  $27.5^\circ\text{S}$ ) (not shown), the energy inertial peak is shifted towards lower frequencies.

The NICs appear to occur preferentially in the southern part of the region we studied (Fig. 8). Currents in the inertial band, with counterclockwise polarization, are detected during 34% of the time north of  $28^\circ\text{S}$  and during 64% of the time south of  $28^\circ\text{S}$ . Using values of rotary coefficient  $r$  as a spectral estimator, the inertial oscillations found in the study area show a clear latitudinal variation (Fig. 8b), with an increased intensity south of  $28^\circ\text{S}$ . Considering  $|r(f)| > 0.75$  as an indicator for near-inertial motion (Thomson et al., 1998), the critical latitude is indeed  $28^\circ\text{S}$ , with the average  $|r|$  larger than 0.75 south of  $28^\circ\text{S}$ . The inertial oscillations are more circularly polarized ( $|r(f)| > 0.75$ ) in the southern part of the region than in the northern part, where  $0.3 < |r(f)| < 0.70$  (Fig. 8b).

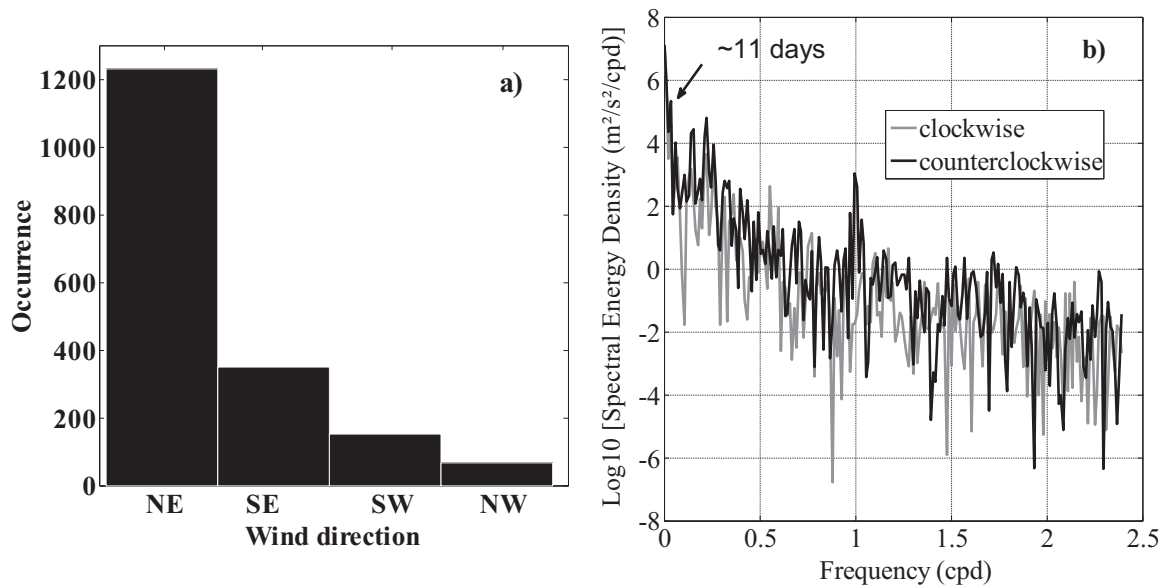


Fig. 4. (a) Histogram of the wind direction, and (b) Energy density rotary spectra of the wind. Period of observation: September to November 2007.

### 3.3. Atmospheric forcing

Synoptic weather charts available at [www.cptec.inpe.br](http://www.cptec.inpe.br) and [www.mar.mil.br](http://www.mar.mil.br), prepared by the Center for Weather Forecasting and Climate Research (CPTEC) of the Brazilian National Institute for Space Research (INPE) and Brazilian Navy, respectively, are analyzed for each NICs event to identify the associated meteorological feature. In a similar way, these analyses are carried out based on the local wind data. The observed features generally fall into three classifications for our study area: 1) cold front; 2) low pressure system; and 3) sea breeze.

#### 3.3.1. Cold front

Pollard (1970) and D’Asaro (1985) show that a strong wind combined with a fairly sudden shift in direction is one of the generation mechanisms of the inertial motions. Stech and Lorenzetti (1992) indicated that during cold fronts, the wind, which in normal conditions blows from the NE in the studied region, rotates counterclockwise and blows from the SW. Based on this criterion, at least 10 cold fronts reach our study area during the experiment (Fig. 9 – upper panel). This result is confirmed by the analysis of available synoptic charts. The excitation

of the near-inertial currents occurred primarily in a small number of short events. As indicated by Stech and Lorenzetti (1992), on average in winter, four cold front events per month reach the study area, with a resultant peak of energy in the wind with a period of approximately 8 days. During the spring season, the number of cold fronts passing through the region is normally lower than in winter. A peak period of 11 days is observed in our wind data (Fig. 4b), that seems to be associated with these events. A wavelet analysis, using a Morlet wavelet with a width of six periods, is applied to identify the wind diurnal energy (Fig. 9 - lower panel). It shows an intense wind diurnal variability between September 30 and October 13. This time window is thus a period of intensified diurnal (breeze) signal.

The injection of energy by the wind prior and after the triggering of the NICs showed in Fig. 8a is investigated in Fig. 10. The sub-panels of Fig. 10 show the simultaneous time series of the wind stress, of the current velocity and of the energy flux from the wind to the currents, as well as the related synoptic chart. As indicated in Fig. 10d, a cold front was present over the drifter set for the period shown in Fig. 8a. The vertical line at 1200 UTC on November 8 denotes approximately the time when the front passed over the region of the drifter trajectories.

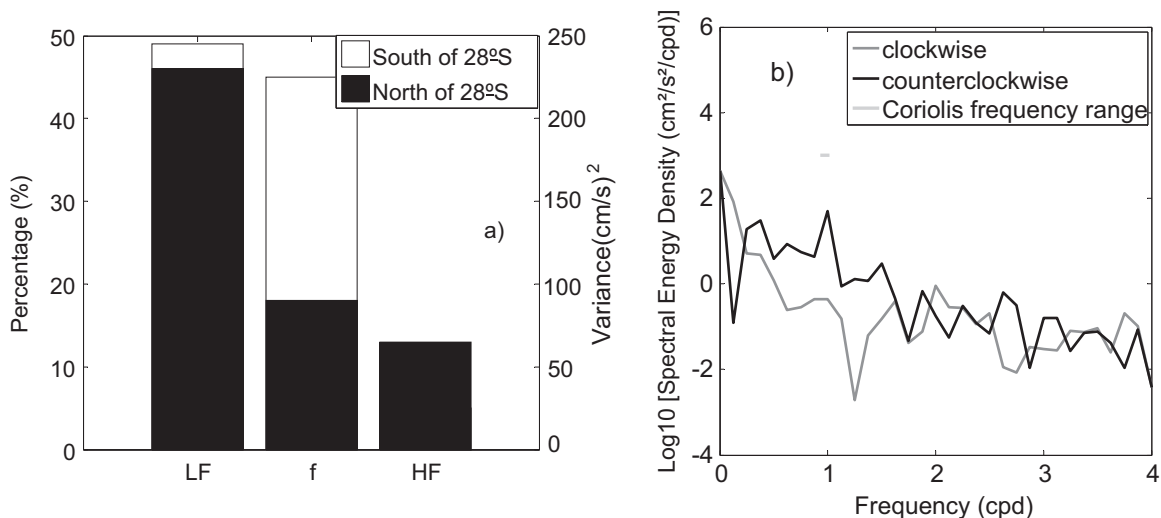


Fig. 5. (a) Band-averaged explained variance for all drifter segments for the latitude band south and north of 28°S, for: low frequency (LF), inertial (f), and high-frequency (HF) bands (same values south and north of 28°S at HF); (b) Typical rotary spectra of current velocity for drifter during inertial oscillation.

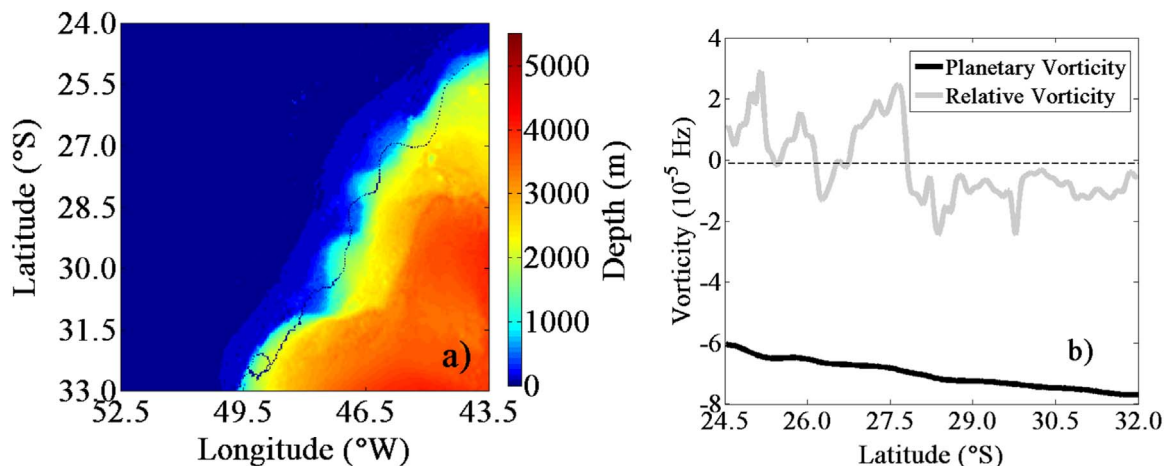


Fig. 6. (a) A typical trajectory followed by the drifters (black line) and the bathymetry (shaded), (b) evolution of  $\zeta$  (gray curve) and  $f$  (black curve) along this trajectory.

The cold front passage over the drifters coincides remarkably with the starting time of inertial motions. The physical processes by which a cold front passage leads to NICs generation is discussed in Section 4.2.

### 3.3.2. Low pressure systems

Some authors (Sinclair, 1995; Hoskins and Hodges, 2005; Reboita et al., 2009) have indicated a large frequency of the low pressure system events off the south/southeastern coast of Brazil. At least one within the twelve meteorological events observed in our dataset is related to some low pressure systems. Rigorously, this meteorological event is related to a combined front-low pressure feature, resulting in a hybrid case (Fig. 11d). Therefore, the generation of inertial currents during this period cannot be associated with a single feature. Like in the case of the cold front passage illustrated in Fig. 10, the generation of NICs on November 10 (Fig. 11b) coincides remarkably with the passage of the cold front-low pressure system. The wind stress power is also very low (less than  $10 \text{ mW m}^{-2}$ ) during the NIC event. In the Southern Hemisphere, the wind associated with the low pressure systems themselves rotates clockwise and therefore it should not force significant inertial currents (Hyder et al., 2007). Thus, much of the

generation of the inertial motions off the south/southeast Brazilian coast should be associated with the passage of cold fronts rather than low pressure systems. The findings of D’Asaro (1985) that large stationary low pressure systems do not excite any inertial oscillations seem to be verified in our study area.

### 3.3.3. Sea breeze

Two periods, October 3 to October 11 and October 31 to November 8, show a strong sea breeze signal (Fig. 9 – upper panel). The synoptic charts indicate that these periods are characterized by the presence of some large stationary pressure systems with a typical lifetime of approximately seven days. During these two periods, the winds blow from the north-east (between  $20^\circ$  and  $50^\circ$  azimuth) (Fig. 12a and Fig. 13a). The wavelet analysis (Fig. 9 – lower panel) shows a large amplitude at the diurnal period in the wind variability, in agreement with a sea breeze signal (Hyder et al., 2007). Furthermore, the rotary spectra of the wind (Fig. 12b and Fig. 13b) reveal maximal amplitudes at the diurnal frequency, with significantly more energy for the counterclockwise component than for the clockwise component. During the clear and warm conditions for the first period (October

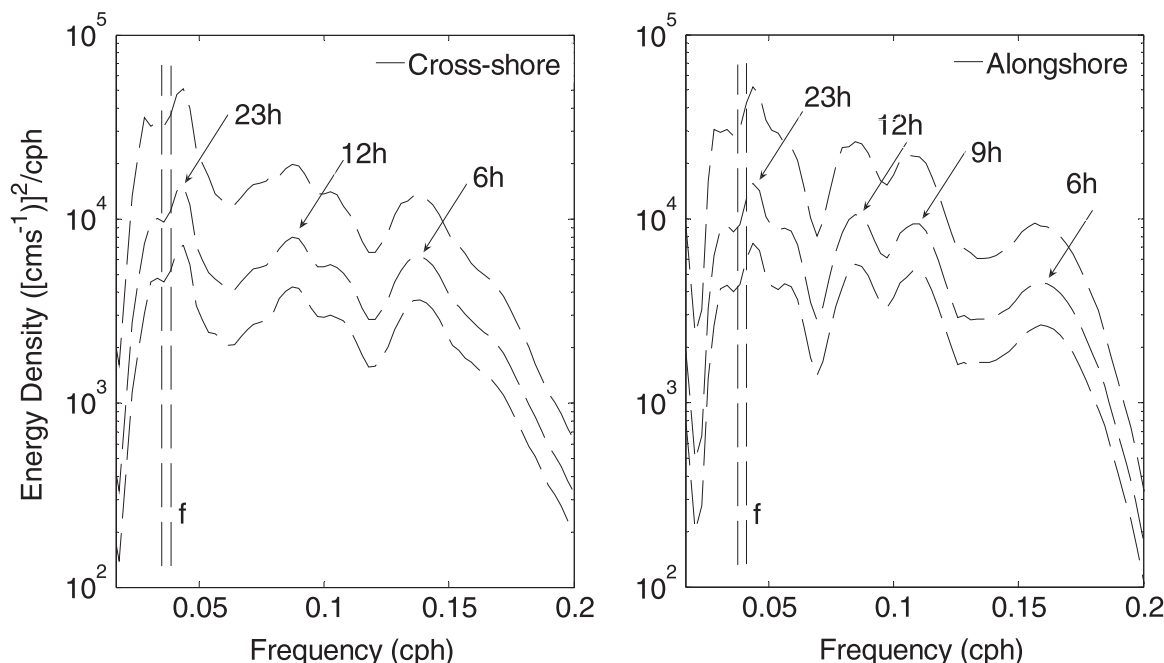
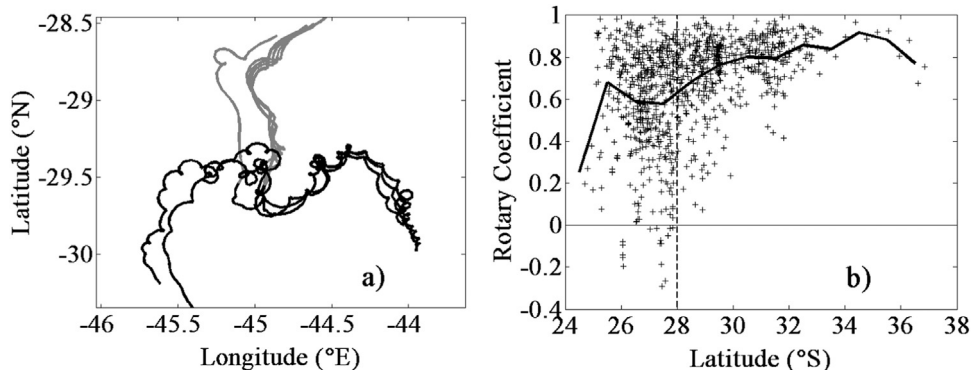
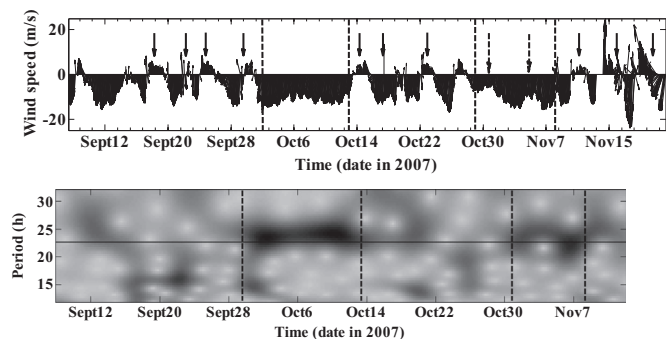


Fig. 7. Spectral analysis of the trajectories south of  $27.5^\circ\text{S}$ . The vertical dashed line indicates the interval for the inertial frequency in the analyzed region (corresponding to periods of 24–26 h); 95% confidence intervals are superimposed.



**Fig. 8.** (a) Typical drifter trajectory before and after the triggering of near-inertial currents: between November 3 and 8 (gray line) and between November 8 and 13 (black line), (b) latitudinal variation of the rotary coefficient at the inertial frequency.



**Fig. 9.** – Wind vector time series (upper panel). Solid arrows show cold front passages. Dashed arrows show cold front passage without wind reversion and dashed lines delimit periods of high diurnal (breeze) variability. Wavelet power spectrum for the cross-shore wind (lower panel).

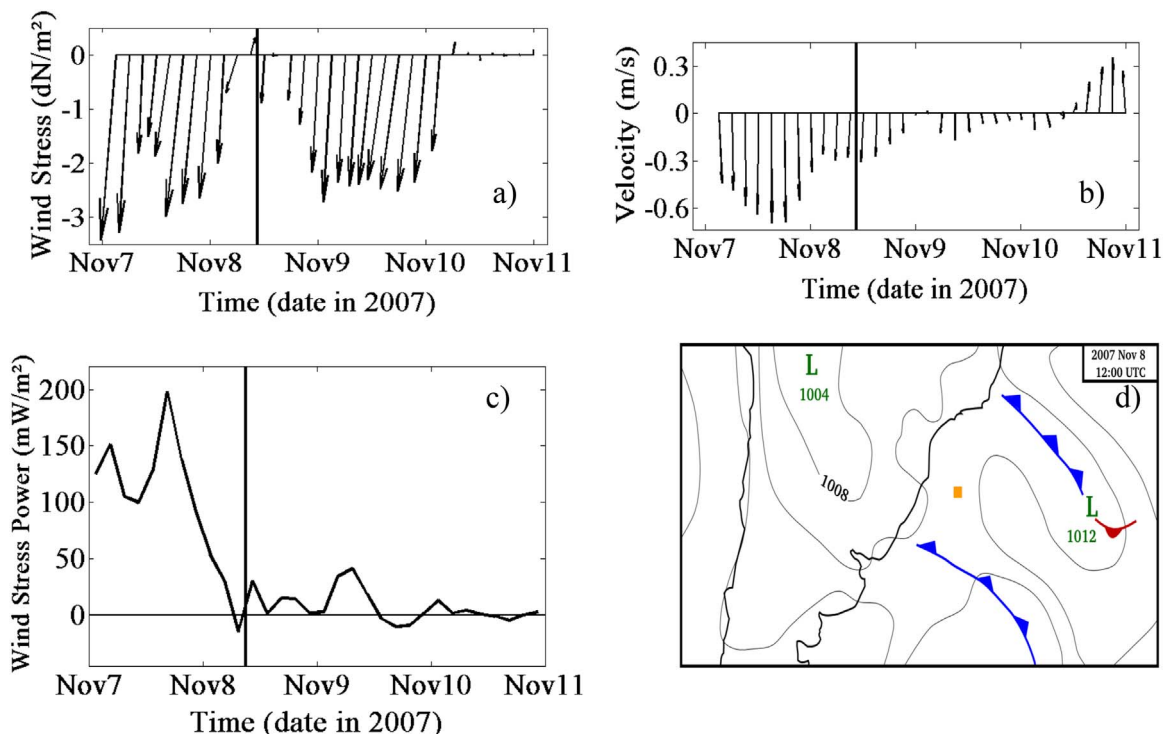


**Fig. 10.** Near-inertial currents between November 7 and November 11, resulting from a cold front passage on November 8: (a) wind stress, (b) drifter velocity, (c) energy flux from the wind to the currents, and (d) synoptic chart on November 8. The yellow box indicates the position of the drifter. The vertical line denotes approximately the time when the front passed over the drifter trajectories (it coincides with the starting time of the near-inertial motions).

3–11), the high-passed (periods shorter than 40 h) time series of cross-shore and along-shore winds show a clear and intense daily cycle (Fig. 12c,d). For the event observed from October 31 to November 8, the daily cycle is also present but with less intensity (Fig. 13c,d).

#### 4. Discussion

We observed an important spatial variability of the near-inertial currents. The 28°S latitude appeared to be a threshold latitude in our region of study, with more frequent and more intense NICs south of it. In the development below, we discuss the physical processes leading to such a variability, the NICs generation mechanisms and the implications for the eddy kinetic energy (EKE).

##### 4.1. The background vorticity contribution

In the studied region the relative vorticity of the background flow shows a counterclockwise tendency (positive vorticity) north of 28°S and a clockwise tendency (negative vorticity) south of it (Fig. 6b). As

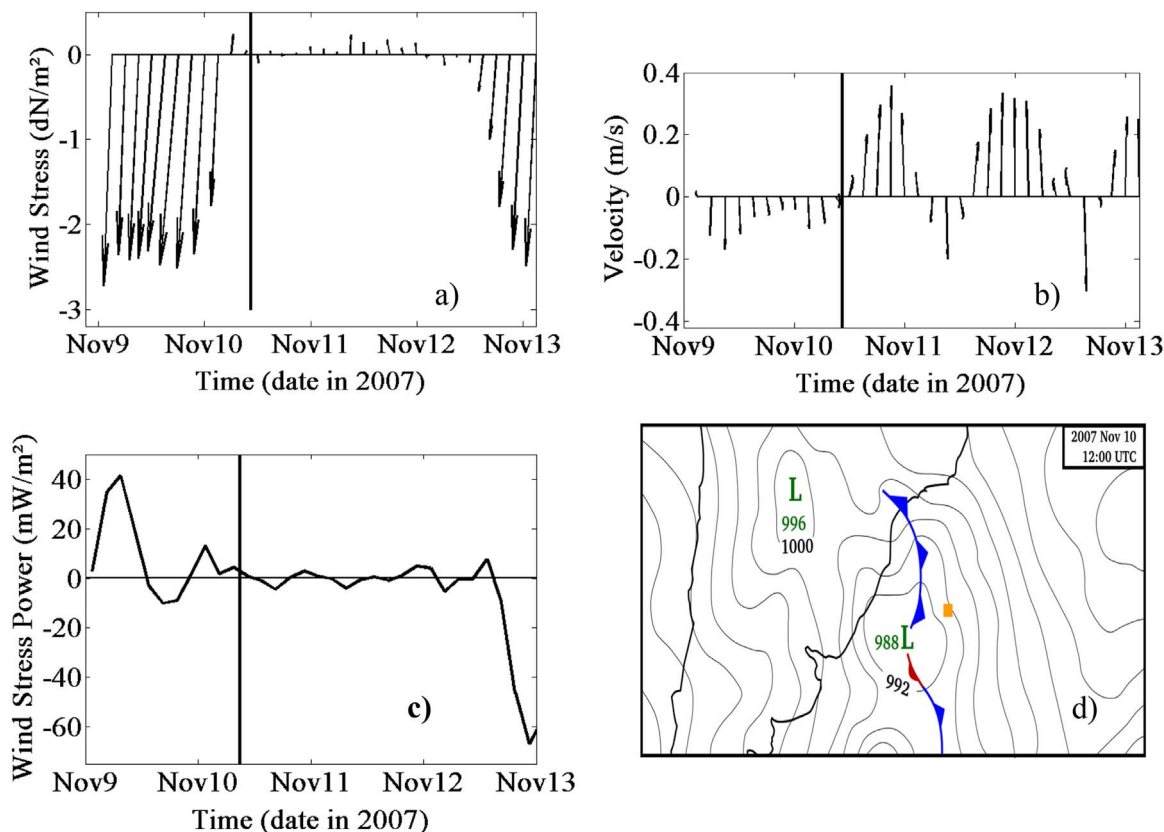


Fig. 11. Near-inertial currents between November 9 and November 13 resulting from a hybrid low pressure system-cold front passage on November 10. (a) – (d) same as in Fig. 10.

indicated by [Elipot et al. \(2010\)](#) regions with large vorticity or large vorticity gradient are associated with large geostrophic EKE. In our study area, the highest EKE was found in the vicinity of 27°S, with values about 612 (cm/s)<sup>2</sup> ([Oliveira et al., 2009](#)). The spectral analysis of trajectories south of 28°S (Fig. 7) indicates that the near-inertial frequency is about 10% higher than the local inertial frequency, a blue frequency shift. Such a shift south of 28°S can be explained by the increase of the absolute value of the Effective Inertial Frequency  $EIF = f + \zeta/2$  ([Kunze, 1985](#)), as the relative vorticity  $\zeta$  is negative like the planetary vorticity  $f$  (Southern Hemisphere). This result confirms that the near-inertial motions south of 28°S are embedded in a cyclonic (negative) vorticity region, as indicated by Fig. 6b.

For the drifter trajectories north of 28°S, there is a shift in the inertial energy peak toward lower frequencies (not shown). As observed by some authors ([Kunze, 1985](#); [Shearman, 2005](#) and [Sobarzo et al., 2007](#), among others), the mean lateral current shear is able to shift down the frequencies, which is a red frequency shift. [Poulain \(1996\)](#) reported a red shift of 0.07 cpd in the inertial frequency for the observations from the North Pacific. Inertial oscillations cannot propagate into positive relative vorticity region because their frequency is higher than the local effective inertial frequency ( $f + \zeta/2$ ). Thus, if embedded in an anticyclonic (positive) vorticity field, some near-inertial motions have intrinsic frequencies lower than the Coriolis frequency, which, for the latitudes in the study area north of 28°S, correspond to periods between 26 and 28 h (diverging from diurnal wind period and avoiding resonance possibility). Another consequence is that the resultant motions have intrinsic frequencies lower than the effective inertial frequency of the surrounding ocean (south of 28°S), so they cannot propagate southward. We speculate that these facts are crucial to explain, despite the favorable wind conditions, the relative few near-inertial movements occurrence observed within the 39 drifters trajectories, in the northern part of the studied region (north of 28°S). These conclusions are similar to those presented by [Pereira](#)

[et al. \(2007\)](#) who showed that the background vorticity has the theoretical potential to reflect, trap, or prohibit the generation of the  $M_2$  internal tide in the South Brazil Bight.

As indicated in Fig. 6b, the relative vorticity shows a clockwise tendency (negative vorticity) south of 28°S. [Shcherbina et al. \(2003\)](#) found a local trapping of near inertial waves by a region of negative relative vorticity associated with the subpolar front in the Japan Sea. [Van Meurs \(1998\)](#), based on surface drifter dataset and the results from a theoretical analysis and some numerical models, stressed the importance of the gradient of vorticity for NICs as their time decay is sped up in regions of high-vorticity gradient.

The observed latitudinal variation of the rotary coefficient at the inertial peak frequency (Fig. 8b) could also be associated with the diurnal atmospheric tide in the surface wind, which, in the region around 30°N/S, may be a major mechanism for atmospheric-ocean transfer ([Stockwell et al., 2004](#)). These authors also found that the surface wind energy at the inertial frequency presents large values at latitudes higher than 30°N/S.

#### 4.2. Generation mechanisms

The relationship of intermittent inertial motions to atmospheric features is investigated by examining some drifter trajectories, the local wind data and some synoptic weather charts in detail. Our focus is to understand what happens before and after the generation of inertial motions (Fig. 8a, gray and black trajectories, respectively).

Cold front is the main generation mechanism of NICs in our study area. Nine out of twelve meteorological events observed are related to some cold fronts. The wind stress vector commonly changes abruptly during a cold front passage (Fig. 10a). This result agrees with [D'Asaro \(1985\)](#) and [Poulain \(1996\)](#) who indicated that near-inertial motions are triggered in the mixed layer by some abrupt wind stress fluctuations. The drifter velocity shows a decay during this period (Fig. 10b). The

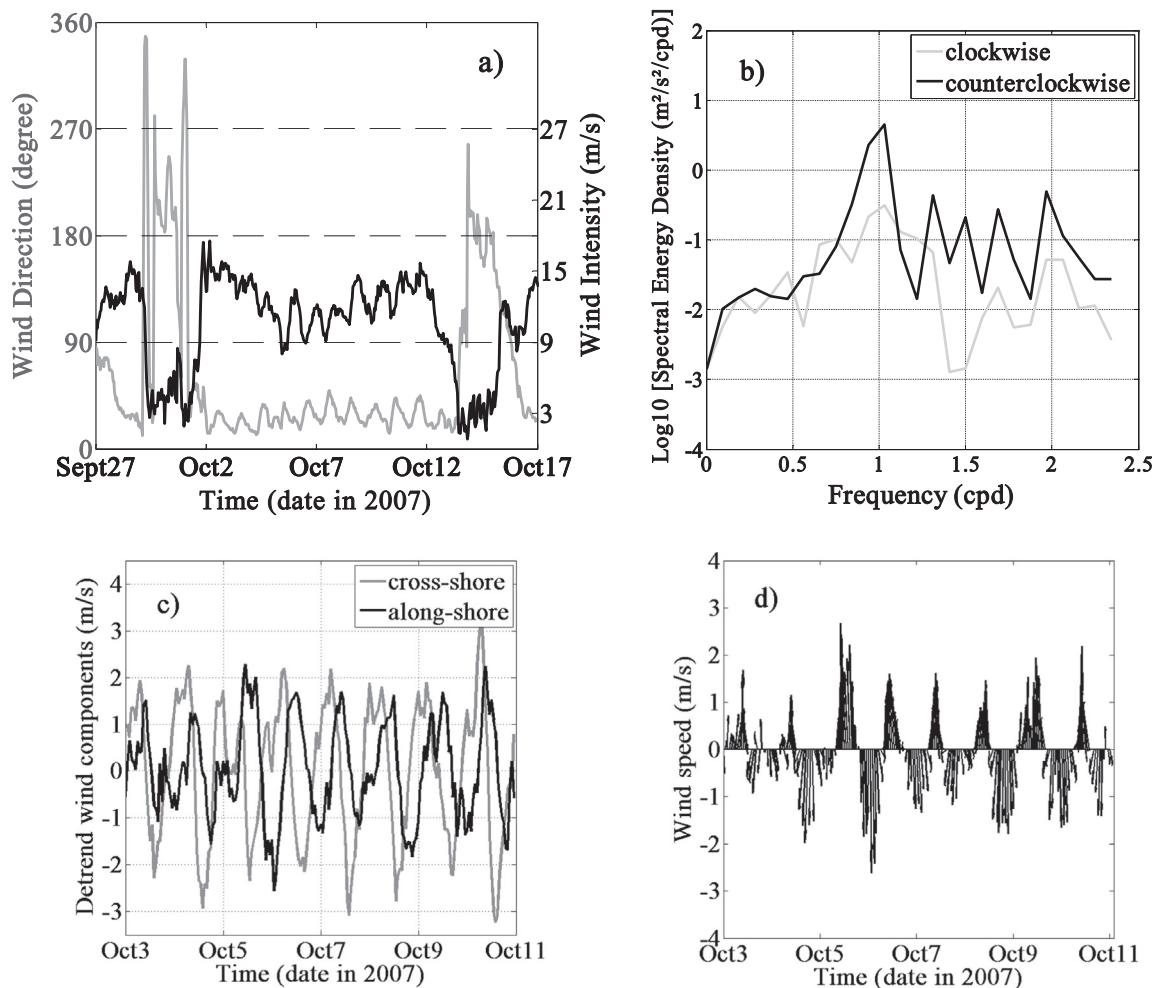


**Fig. 12.** (a) Wind direction (gray) and amplitude (black) from October 3 to October 11. (b) Rotary spectra of filtered wind during the same period. (c) Wind components of filtered wind. (d) Stick representation of filtered wind. Positive values are directed eastward and northward.

flux of energy from the wind to the surface current has been estimated from the wind stress and the ocean currents velocity measured by mooring (D'Asaro, 1985), from global wind stress analyses (Watanabe and Hibiya, 2002; Alford, 2003a, 2003b), or more recently, from surface drifter data (Elipot and Gille, 2009). The flux of energy during the analyzed period, computed here as the dot product between the wind stress and the drifter velocity, falls from 200 mW m<sup>-2</sup> to less than 40 mW m<sup>-2</sup> after the cold front passage, and it stays very low onward (Fig. 10c). As pointed out by Pollard (1980) and D'Asaro (1985) the wind can both accelerate and decelerate the inertial currents. In our case, the wind stress during the cold front passage (dominantly from southwest) opposes the surface current (dominantly from the northeast), resulting in a short period of negative values for the wind stress power. Here, the occurrence of the near-inertial motions in the Brazil Current seems thus to be associated with a loss of energy. The downward transport of energy toward the ocean interior by some propagating internal waves can also contribute to the loss of energy of the surface layer, as observed by D'Asaro et al. (1995) in the northeast Pacific Ocean.

#### 4.3. Resonant forcing

Our observations of the sea breeze around the SE/S Brazilian shelf break in spring showed a velocity amplitude about 2 m s<sup>-1</sup>, half of the value (~4 m s<sup>-1</sup>) observed by Zhang et al. (2010) in the Gulf of Mexico, considered to be a strong sea breeze. These authors indicated that at 30°N (critical latitude), this sea breeze is able to deepen the 15 °C

isotherm from 15 m to 25 m. This strong effect is produced because the sea breeze is resonant with the inertial period of the ocean at 30°N/S (Hyder et al., 2007).

The sea breeze is known to produce near-inertial currents (Pollard, 1970; Pollard and Millard, 1970; Rippeth et al., 2002; Hyder et al., 2007; Hyder et al., 2011). In our case, north-easterly wind, fluctuating at the diurnal frequency due to a spring breeze regime, is a candidate for driving the diurnal motions, as shown by the drifters during the October 3–11 period (Fig. 14a). This process occurred in a region of concave coastline curvature (Fig. 1a) which can cause the convergence of the land breeze (Neumann, 1951; Arritt, 1989), enhancing the breeze regime contributions to the near-inertial motions.

For this sea breeze period (between the vertical lines in Fig. 14b), a sharp decrease is observed in the wind stress power and, typically, an oscillating pattern between the negative and positive values is found during this period. Nevertheless, the inertial peak amplitude is more pronounced (gray curve in Fig. 14b). Thus, it seems that the oscillatory pattern in the wind stress power, rather than its amplitude, is more important to enhance the inertial motions in our study region. As suggested by DiMarco et al. (2000), some near-inertial currents can be excited by a weak, fluctuating wind, during some favorable conditions for resonance effect: the frequency and the phase acting for the reinforcement. An example of this is given in Fig. 14b between October 2 and October 10 and in Fig. 15b, between November 3 and November 8. In both cases, the inertial current intensity continues to increase while the wind stress power declined.

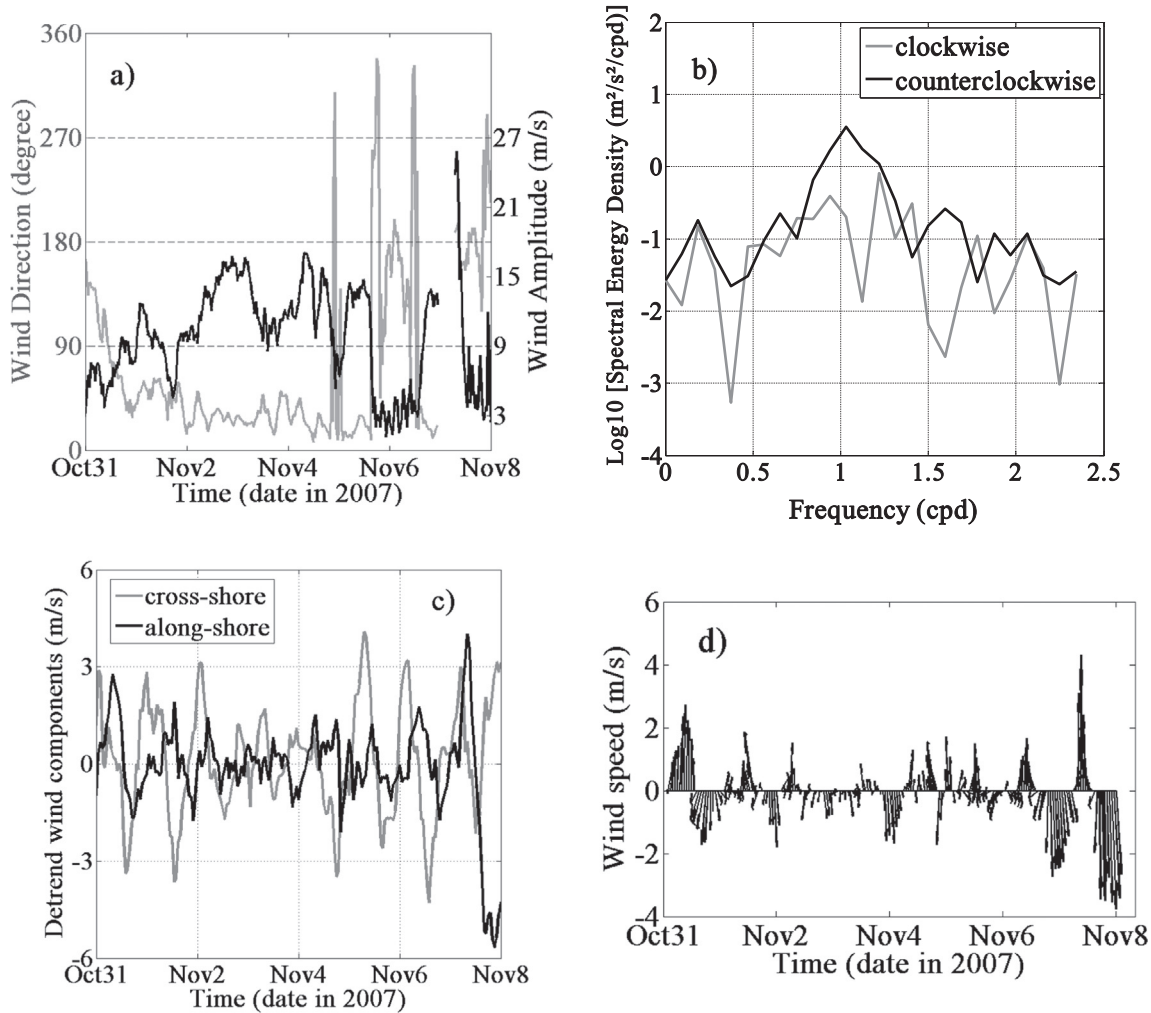


Fig. 13. (a-d) same as Fig. 12 for the period from October 31 to November 8.

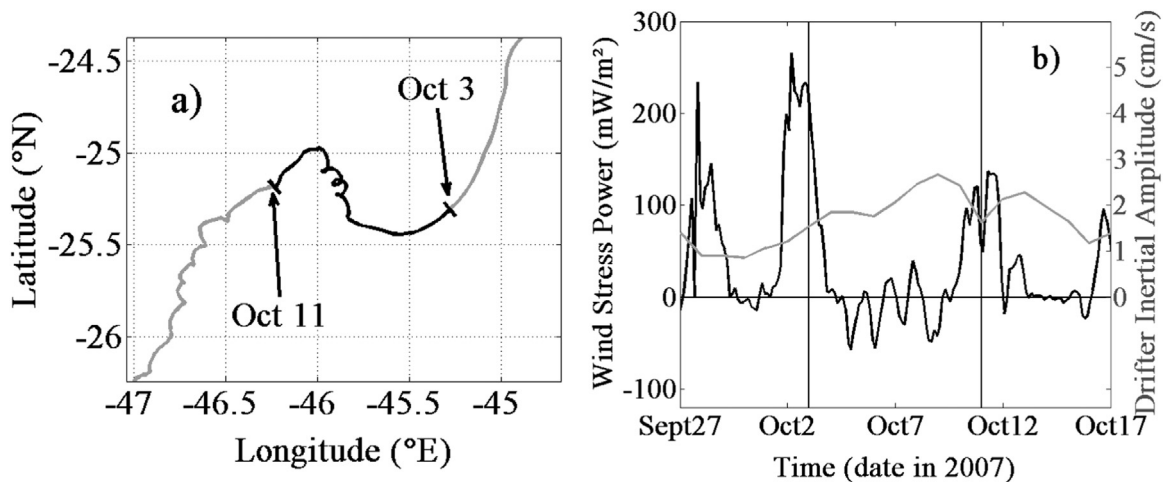
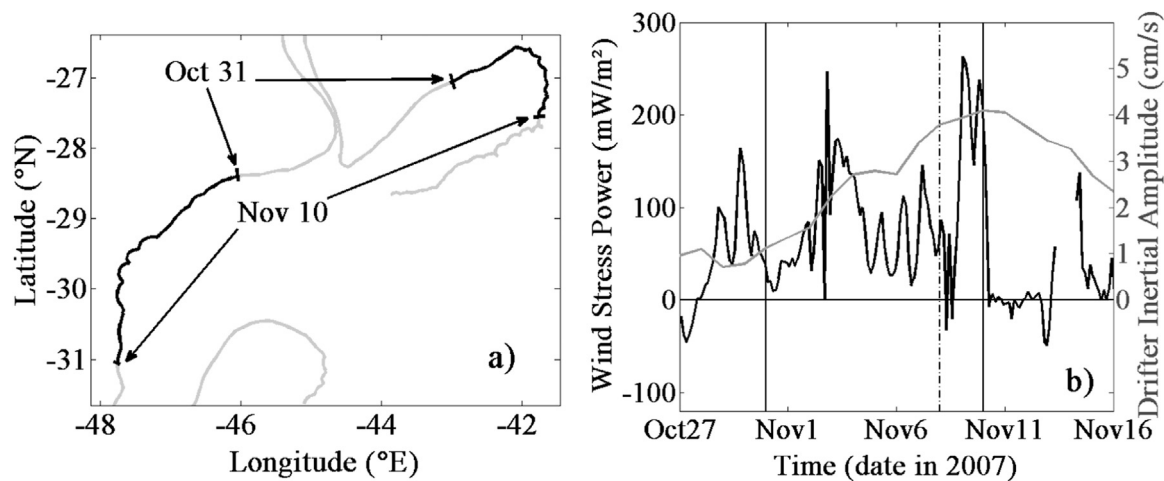


Fig. 14. (a) Drifter trajectory showing near-inertial oscillations during the first period of intense breeze signal (October 3 to October 11) and (b) energy flux from the wind stress to the ocean current (black) and inertial peak amplitude of the current (gray) The solid lines represent the dates of October 3 and October 11, 2007.

4.4. Implications for EKE

The dramatic latitudinal increase in the percentage of the explained variance in the *f* band [18% (north of 28°S) to 45% (south of 28°S)] (Fig. 5a), is seen to be associated with the strength and the sense of the rotary submesoscale motions observed in this region (Fig. 8b). The presence of a rich and energetic submesoscale field, with *O*(1) Rossby,

can alter the EKE by as much as a factor of two (Sasaki et al., 2014; Qiu et al., 2014), a result consistent with the latitudinal EKE variation in the *f* band observed here. The prevailing EKE estimates along BC (Assireu et al., 2003; Assireu, 2003; Oliveira et al., 2009) neglected the importance of the submesoscale flow, which was previously removed during the temporal filtering process. Our findings here indicate that such results should, therefore, be revisited, specially for estimates done south of 28°S.



**Fig. 15.** (a) Two drifter trajectories showing near-inertial oscillations during the second breeze period (October 31 to November 10), and (b) energy flux from the wind stress to the ocean current (black) and the inertial peak amplitude of this drifter (gray). The solid lines represent the date of October 31 and November 10 and the dashed-dotted line represents the date of November 8, just before the wind reversion.

In a recent analysis of the relative drifter dispersion in the south-western Atlantic, [Berti et al. \(2011\)](#) indicated that the submesoscale features were important to determine the dispersion and the shape of the energy spectrum. However, they did not take into account the strong spatial variability in the submesoscale activity relatively to the 28°S latitude reported here. As anticipated by [Thomas et al. \(2008\)](#), and later confirmed by [Haza et al. \(2012\)](#), the presence of an energetic submesoscale field, of  $O(1)$  Rossby, has a significant impact on the structure of the mixed layer and it significantly enhances the lateral dispersion of any passive tracers. Thus, we can expect that the strong change in the EKE related to the inertial frequency south of 28°S presents the potential to influence the results of relative dispersion and the energy spectrum shown by [Berti et al. \(2011\)](#).

## 5. Summary

Observations of wind and surface drifter trajectories show that near-inertial currents are common around the Brazilian southeast-south continental shelf break, where these currents have amplitudes as large as  $30 \text{ cm s}^{-1}$ . The rotary spectral analysis shows that the wind stress is counterclockwise polarized with a pronounced near-inertial peak, which is favorable to force near-inertial currents in the Southern Hemisphere. The motions in the  $f$  band account for 18% of the variance north of the 28°S latitude (the transition zone between positive and negative relative vorticity) and for 45% of the variance south of 28°S. The spatial distributions of the rotary coefficient, which indicates the strength and sense of the rotary motions, indicates that the near-inertial currents in the southern portion of the domain (south of 28°S) are more circularly polarized than those in the northern portion. As anticipated by [Elipot et al. \(2010\)](#), the space variability of NICs is affected by the background vorticity. The temporal decay of the NICs is sped up in the regions with high vorticity gradient, as observed north of 28°S. This unfavorable impact of the background vorticity explains the relatively few NICs occurrences in the northern portion of the domain (north of 28°S), even when the wind conditions are favorable.

Several authors have suggested that the NICs intermittency may be related to the background vorticity. In our case, the relative vorticity ranges from  $-0.3f$  to  $+0.4f$ . There is counterclockwise (anticyclonic, positive) vorticity in the northern portion of our study area and clockwise (cyclonic, negative) vorticity in the southern portion. The cyclonic relative vorticity shifts the effective inertial frequency towards the diurnal frequency, making the southern portion of the study area favorable to the resonance of the current response to the diurnal wind forcing.

The near-inertial motions in the study area are also effectively generated by the shifting of the wind associated with the passages of cold fronts and by the diurnal atmospheric forcing (sea breeze). Nine out of twelve events observed are related to some cold fronts. The near-inertial currents forced by the sea breeze are related to some large stationary pressure systems with a lifetime of approximately seven days. The concave coastline curvature between 24°S and 28°S, which can cause convergence of the land breeze ([Neumann, 1951](#); [Arritt, 1989](#)) and the proximity with the critical latitude of 28°S, are expected to enhance the breeze contribution to the triggering of the near-inertial currents.

The results of this paper highlight the large increase in the eddy kinetic energy in the  $f$  band south of 28°S. As a result, the previous studies on the kinetic energy in the study area have to be revisited since their time window filtering and 6 h subsampling may have impacted the submesoscale energy in their results. As stressed by [D'Asaro \(1985\)](#), for a given forcing amplitude, the shallower the mixed layer is, the more intense the induced near-inertial motions should be. Therefore, the incorporation of the seasonal cycle of the stratification and of the mixed-layer depth in the studied region should provide useful information about the seasonal cycle of the near-inertial motions.

## Acknowledgments

We would like to thank PROOCEANO and Eni Oil do Brasil S.A. for making this valuable data set available for scientific research. A. T. Assireu acknowledges support from CNPq (309315/2015-8) and FAPEMIG (APQ 1458-14). The authors would like to thank two anonymous reviewers for constructive criticisms, Dr. Felipe Mendonça Pimenta for his critical review of this manuscript and Chloe Furnival for text review.

## References

- Alford, M., 2003a. Improved global maps and 54-year history of wind work on ocean inertial motions. *Geophys. Res. Lett.* 30. <http://dx.doi.org/10.1029/2002GL016614>.
- Alford, M., 2003b. Redistribution of energy available for ocean mixing by long range propagation of internal waves. *Nature* 423, 159–162.
- Alford, M., Cronin, M., Klymak, J., 2012. Annual cycle and depth penetration of wind-generated near-inertial internal waves at ocean station papa in the Northeast Pacific. *J. Phys. Oceanogr.* 42, 889–909.
- Arthur, R.S., 1965. On the calculation of vertical motion in eastern boundary currents from determinations of horizontal motion. *J. Geophys. Res.* 70 (12), 2799–2802.
- Arritt, R., 1989. Numerical modeling of the offshore extent of sea breezes. *Q. J. R. Meteorol. Soc.* 115, 547–570.
- Assireu, A.T., 2003. Estudo das características cinemáticas e dinâmicas das águas de superfície do Atlântico Sul Ocidental a partir de derivadores rastreados por satélite

- (Ph.D. Thesis). Oceanographic Institute, University of São Paulo, (174 pp).
- Assireu, A.T., Stevenson, M.R., Stech, J.L., 2003. Surface circulation and kinetic energy in the SW Atlantic obtained by drifters. *Cont. Shelf Res.* 23, 145–157.
- Berti, S., Santos, F.A., Lacorata, G., Vulpiani, A., 2011. Lagrangian drifter dispersion in the Southwestern Atlantic Ocean. *J. Phys. Oceanogr.* 41, 1659–1672.
- Castro Filho, B.M., Lorenzetti, J.A., Silveira, I.C.A., Miranda, L.B., 2006. Estrutura termohalina e circulação na região entre o Cabo de São Tomé (RJ) e o Chuí (RS). O Ambiente Oceanográfico da Plataforma Continental e do Talude na Região Sudeste-Sul do Brasil. C.L.D.B. Rosi-Wongtschowski and L.S.P. Madureira, Eds., Edusp, 11–120.
- Chen, C., Xie, L., 1997. A numerical study of wind-induced, near-inertial oscillations over the Texas-Louisiana shelf. *J. Geophys. Res.* 102 (C7), 15 583–15 593.
- Crawford, G.B., Large, W.L., 1996. A numerical investigation of resonant inertial response of the ocean to wind events. *J. Phys. Oceanogr.* 26, 873–891.
- Crawford, W.R., Cherniawsky, J.Y., Foreman, G.G., 1997. Rotary velocity spectra from short drifter tracks. *J. Atmos. Ocean. Technol.* 15, 731–740.
- D'Asaro, E., 1985. The energy flux from the wind to near-inertial motions in the surface mixed layer. *J. Phys. Oceanogr.* 15, 1043–1059.
- DiMarco, S.F., Howard, M.K., Reid, R.O., 2000. Seasonal variation of wind-driven current cycling on the Texas Louisiana continental shelf. *Geophys. Res. Lett.* 27 (7), 1017–1020.
- Elipot, S., Lumpkin, R., Prieto, G., 2010. Modification of inertial oscillations by the mesoscale eddy field. *J. Geophys. Res.* 115, C09010, (20p).
- Elipot, S., Gille, S.T., 2009. Estimates of wind energy input to the Ekman layer in the Southern Ocean from surface drifter data. *J. Geophys. Res.* 114, C06003, (14p).
- Franchito, S.H., Rao, V.B., Stech, J.L., Lorenzetti, J.A., 1998. The effect of coastal upwelling on the sea-breeze circulation at Cabo Frio, Brazil: a numerical experiment. *Ann. Geophys.* 16, 866–881.
- Furuichi, N., Hibiya, T., Niwa, Y., 2008. Model predicted distribution of wind-induced internal wave energy in the world's oceans. *J. Geophys. Res.* 113, C09034. <http://dx.doi.org/10.1029/2008JC004768>.
- Gill, A.E., 1984. On the behavior of internal waves in the wake of a storm. *J. Phys. Oceanogr.* 14, 1129–1151.
- Gille, S.T., Llewellyn-Smith, S.G., Lee, S.M., 2003. Measuring the sea breeze from QuickSCAT scatterometry. *Geophys. Res. Lett.* 30, 1114. <http://dx.doi.org/10.1029/2002GL016230>.
- Gille, S.T., Llewellyn-Smith, S.G., Stom, N.M., 2005. Global observations of the land breeze. *Geophys. Res. Lett.* 32 (5). <http://dx.doi.org/10.1029/2004GL022139>.
- Gonella, J., 1972. A rotary-component method for analysing meteorological and oceanographic vector time series. *Deep-Sea Res.* 19, 833–846.
- Gordon, A., Greengrove, C., 1986. Geostrophic circulation of the Brazil-Falkland confluence. *Deep-Sea Res.* 33A, 573–585.
- Haza, A.C., Özgökmen, T.M., Griffa, A., Garaffo, Z.D., Piterberg, L., 2012. Parameterization of particle transport at submesoscales in the Gulf Stream region using Lagrangian subgridscale models. *Ocean Model.* 42, 31–49.
- Hansen, D., Poulain, P., 1996. Quality control and interpolations of WOCE-TOGA drifter data. *J. Atmosph. Ocean Tech.* 13, 900–909.
- Hoskins, B.J., Hodges, K.L., 2005. A new perspective on Southern Hemisphere storm tracks. *J. Climatol.* 18, 4108–4129.
- Houry, S., Drombowski, P., Mey, D., Minster, J., 1987. Brunt-Väisälä frequency and Rossby radii in the South Atlantic. *J. Phys. Oceanogr.* 17, 1619–1626.
- Hyder, P., Simpson, J.H., Christopoulos, S., 2007. Sea breeze forced diurnal surface current in the Thermaikos Gulf, North-west Aegean. *Cont. Shelf Res.* 22, 585–601.
- Hyder, P., Simpson, J.H., Xing, J., Gille, S.T., 2011. Observations over an annual cycle and simulations of wind-forced oscillations near the critical latitude for diurnal-inertial resonance. *Cont. Shelf Res.* 31, 1576–1591.
- Jarosch, E., Hallock, Z.R., Teague, W.J., 2007. Near-inertial currents in the DeSoto Canyon region. *Cont. Shelf Res.* 27, 2407–2426.
- Kroll, J., 1975. The propagation of wind-generated inertial oscillations from the surface to the deep ocean. *J. Mar. Res.* 33, 15–51.
- Kunze, E., 1985. Near-inertial wave propagation in geostrophic shear. *J. Phys. Oceanogr.* 15, 544–565.
- Lima, I.D., Garcia, C.A.E., Möller, O.O., 1996. Ocean surface processes on the southern Brazilian shelf: characterization and seasonal variability. *Cont. Shelf Res.* 16, 1307–1317.
- Lorenzetti, J.A., Stech, J.L., MeloFilho, W.L., Assireu, A.T., 2009. Satellite observation of Brazil Current inshore thermal front in the SW South Atlantic: space/time variability and sea surface temperatures. *Cont. Shelf Res.* 29, 2061–2068.
- Mesquita, A.R., Harari, J., 2003. On the harmonic constants of tides and tidal currents of the South-eastern Brazilian shelf. *Cont. Shelf Res.* 23, 1227–1237.
- Müller, T.J., Ikeda, Y., Zangenberg, N., Nonato, L.V., 1998. Direct measurements of western boundary currents off Brazil between 20°S and 28°S. *J. Geophys. Res.* 103 (C3), 5429–5437.
- Munk, W., Wunsch, C., 1998. Abyssal recipes II: energetics of tidal and wind mixing. *Deep-Sea Res.* 45, 1977–2010.
- Nakamura, M., Kagimoto, T., 2006. Potential vorticity and eddy potential enstrophy in the North Atlantic Ocean simulated by a global eddy-resolving model. *Dyn. Atmos. Oceans* 41, 28–59.
- Neumann, J., 1951. Land Breeze and nocturnal thunderstorms. *J. Meteorol.* 8, 60–67.
- Oliveira, L.R., Piola, A.R., Mata, M.M., Soares, I.D., 2009. Brazil current surface circulation and energetics observed from drifting buoys. *J. Geophys. Res.* 114, C10006. <http://dx.doi.org/10.1029/2008JC004900>.
- Park, J., Kim, K., King, B., 2005. Global statistics of inertial motions. *Geophys. Res. Lett.* 32, 1–5. <http://dx.doi.org/10.1029/2005GL023258> (L14612).
- Pattiaratchi, C., Hegge, B., Gould, J., Eliot, I., 1997. Impact of sea-breeze activity on nearshore and foreshore processes in southwestern Australia. *Cont. Shelf Res.* 17, 1539–1560.
- Pereira, A.F., Castro, B.M., Calado, L., da Silveira, I.C.A., 2007. Numerical simulation of M2 internal tides in the South Brazil Bight and their interaction with the Brazil Current. *J. Geophys. Res.* 112, C04009. <http://dx.doi.org/10.1029/2006JC003673>.
- Peterson, R.G., Stramma, L., 1991. Upper-level circulation in the South Atlantic Ocean. *Progr. Oceanogr.* 26, 1–73.
- Pollard, R.T., 1970. On the generation by winds of inertial waves in the ocean. *Deep-Sea Res.* 17, 795–812.
- Pollard, R.T., 1980. Properties of near-surface Inertial Oscillations. *J. Phys. Oceanogr.* 10, 385–397.
- Poulain, P.M., 1996. Near-inertial and diurnal motions in the trajectories of mixed layer drifters. *J. Marine Res.* 48, 793–823.
- Price, J.F., 1981. On the upper ocean response to a moving hurricane. *J. Phys. Oceanogr.* 11, 153–175.
- Qiu, B., Chen, S., Klein, P., Sasaki, H., Sasai, Y., 2014. Seasonal mesoscale and submesoscale eddy variability along the North Pacific subtropical Counter current. *J. Phys. Oceanogr.* 44 (12), 3079–3098. <http://dx.doi.org/10.1175/JPO-D-14-0071.1>.
- Reboita, M.S., Rocha, R.P., Ambrizzi, T., Sugahara, S., 2009. South Atlantic Ocean cyclogenesis climatology simulated by regional climate model (RegCM3). *Climatol. Dyn.* 35, 1331–1347.
- Rippeth, T.P., Simpson, J.H., Player, R.J., Garcia, M., 2002. Current oscillations in the diurnal inertial band on the Catalanian Shelf in Spring. *Cont. Shelf Res.* 22, 247–265.
- Sasaki, H., Klein, P., Qiu, B., Sasai, Y., 2014. Impact of oceanic-scale interactions on the seasonal modulation of ocean dynamics by the atmosphere. *Nat. Commun.* 5, 1–8. <http://dx.doi.org/10.1038/ncomms6636>, (Publisher's official version).
- Shcherbina, A.Y., Talley, L.D., Firing, E., Hacker, P., 2003. Near-surface frontal zone trapping and deep upward propagation of internal wave energy in the Japan/East Sea. *J. Phys. Oceanogr.* 33, 900–912.
- Shearman, R.K., 2005. Observations of near-inertial current variability on the new England Shelf. *J. Geophys. Res.* 110 (C2), 902–919.
- Silveira, I.C.A., Schmidt, A.C.K., Campos, E.J.D., de Godoi, S.S., Ikeda, Y., 2000. The Brazil current off the eastern Brazilian coast. *Rev. Bras. Oceanogr.* 48 (2), 171–183.
- Simpson, J.H., Hyder, P., Rippeth, T.P., Lucas, I., 2002. Forced oscillations near the critical latitude for diurnal inertial resonance. *J. Phys. Oceanogr.* 32, 177–187.
- Sinclair, M.R., 1995. A climatology of cyclogenesis for the southern hemisphere. *Mon. Weather Rev.* 123, 1601–1619.
- Sobarzo, M., Shearman, R.K., Lentz, S., 2007. Near-inertial motions over the continental shelf off Concepción, central Chile. *Progr. Oceanogr.* 75, 348–362.
- Souza, R.B., Robinson, L., 2003. Lagrangian and satellite observations of the Brazilian Coastal Current. *Cont. Shelf Res.* 24, 241–262.
- Stech, J.L., Lorenzetti, J.A., 1992. The response of the south Brazil bight to the passage of wintertime cold fronts. *J. Geophys. Res.* 97 (C6), 9507–9520.
- Stevenson, M.R., Dias-Brito, D., Stech, J.L., Kampel, M., 1998. How do cold water biota arrive in a tropical bay near Rio de Janeiro, Brazil? *Cont. Shelf Res.* 18, 1595–1612.
- Stockwell, R., Large, W., Milliff, R., 2004. Resonant inertial oscillations in moored buoy ocean surface winds. *Tellus* 56A, 536–547.
- Sybrandy, A.L., Niiler, P.P., 1991. WOCE/TOGA Lagrangian Drifter-construction Manual. University of California, (92p).
- Thomas, L.N., Tandon, A., Mahadevan, A., 2008. Submesoscale processes and dynamics. In: Hecht, M.W., Hasumi, H. (Eds.), *Eddy Resolving Ocean Modeling*. American Geophysical Union, 17–38.
- Thomson, R.E., LeBlond, P.H., Rabinovich, A.B., 1998. Satellite-tracked drifter measurement of inertial and semidiurnal currents in the northeast Pacific. *J. Geophys. Res.* 103 (C1), 1039–1052.
- Van Meurs, P., 1998. Interactions between near-inertial mixed layer currents and the mesoscale: the importance of spatial variabilities in the vorticity field. *J. Phys. Oceanogr.* 28 (7), 1363–1388. [http://dx.doi.org/10.1175/1520-0485\(1998\)028<1363:IBNIML>2.0.CO;2](http://dx.doi.org/10.1175/1520-0485(1998)028<1363:IBNIML>2.0.CO;2).
- Watanabe, M., Hibiya, T., 2002. Global estimates of the wind-induced energy flux to inertial motions in the surface mixed layer. *Geophys. Res. Lett.* 29 (8). <http://dx.doi.org/10.1029/2001GL014422>.
- Xing, J., Davies, A.M., Fraunie, P., 2004. Model studies of near-inertial motion on the continental shelf off northeast Spain: a three-dimensional/two-dimensional/one-dimensional model comparison study. *J. Geophys. Res.* 109, C01017. <http://dx.doi.org/10.1029/2003JC001822>.
- Zhang, X., Smith, D.C., IV, DiMarco, S.F., Hetland, R.D., 2010. A numerical study of sea-breeze-driven ocean Poincaré wave propagation and mixing near the critical latitude. *J. Phys. Oceanogr.* 40, 48–66.